© 2018. Published by The Company of Biologists Ltd | Journal of Experimental Biology (2018) 221, jeb172312. doi:10.1242/jeb.172312

RESEARCH ARTICLE

Intrinsic curvature in wool fibres is determined by the relative length of orthocortical and paracortical cells

Duane P. Harland[1,*], James A. Vernon[1], Joy L. Woods[1], Shinobu Nagase[2], Takashi Itou[2], Kenzo Koike[2,*], David A. Scobie[3], Anita J. Grosvenor[1], Jolon M. Dyer[1] and Stefan Clerens[1]

ABSTRACT

Hair curvature underpins structural diversity and function in mammalian coats, but what causes curl in keratin hair fibres? To obtain structural data to determine one aspect of this question, we used confocal microscopy to provide *in situ* measurements of the two cell types that make up the cortex of merino wool fibres, which was chosen as a well-characterised model system representative of narrow diameter hairs, such as underhairs. We measured orthocortical and paracortical cross-sectional areas, and cortical cell lengths, within individual fibre snippets of defined uniplanar curvature. This allowed a direct test of two long-standing theories of the mechanism of curvature in hairs. We found evidence contradicting the theory that curvature results from there being more cells on the side of the fibre closest to the outside, or convex edge, of curvature. In all cases, the orthocortical cells close to the outside of curvature were longer than paracortical cells close to the inside of the curvature, which supports the theory that curvature is underpinned by differences in cell type length. However, the latter theory also implies that, for all fibres, curvature should correlate with the proportions of orthocortical and paracortical cells, and we found no evidence for this. In merino wool, it appears that the absolute length of cells of each type and proportion of cells varies from fibre to fibre, and only the difference between the length of the two cell types is important. Implications for curvature in higher diameter hairs, such as guard hairs and those on the human scalp, are discussed.

KEY WORDS: Hair, Wool, Single-fibre curvature, Orthocortex, Paracortex, Cortical cells

INTRODUCTION

Hair, along with milk production, is a definitive phenotypic trait for mammals. Hair appears to have evolved from scales of synapsid reptiles around 200-million years ago (Alibardi, 2006; Maderson, 2003), and hair was already a well-established trait at the very dawn of mammalian evolution because most aspects of hair biology are highly conserved across all existing mammals, including general fibre morphology.

Mammalian coats are typically composed of mixtures of differently functional hair types that are arranged in a three-dimensional (3D) structure, or pelage. The emergent properties of the pelage, and its modification over time (typically seasonal), forms the functional phenotype upon which evolutionary selection occurs, and the adaptability of which has enabled mammals to colonise a wide range of habitats, including climatic extremes (Ryder, 1973). In a typical pelage, for example that of a deer, straight high-diameter guard hairs scaffold a mass of narrow diameter curly underhairs (Brunner and Coman, 1974; Woods et al., 2011), with the combined effect of thermoregulation and mechanical protection. Single-fibre properties, in particular length, diameter and curvature, are important in defining the emergent properties of the pelage. The underpinning mechanism that connects structures at the protein and microstructure level to single-fibre curvature is not well resolved. Here, we use merino wool as a model for understanding the basis of mammalian hair curvature. Whereas wild sheep have a typical pelage of high diameter guard hairs and low diameter underhairs, in that of merino domestic sheep, both guard and underhairs have been selected to be of low diameter and high curvature (Harland et al., 2015; Ryder, 1964).

It has long been known that, in wool fibres, there is an approximate correlation between the amounts and distributions of different wool cortical cell types and fleece crimp [the primary parameter of the sheep pelage structure, observed as a wave within a clipped staple (tress/tuft) of wool typically containing thousands of fibres]. Crimp is an emergent effect of single-fibre curvature. Fibre curvature is of two sorts: intrinsic curvature and imposed curvature. Intrinsic curvature is built into a fibre during its development in the follicle, and it is this curvature, sometimes called inherent curvature, to which an undamaged fibre returns when relaxed in water and dried without mechanical constraint (Fish et al., 1999). Imposed curvature is any chemically or physically induced change to intrinsic curvature; for example, from drying a fibre in a constrained state. Here, we investigate intrinsic curvature (Fig. S1).

The observation that high-crimp wools tend to have a cortex in which the cell types are bilaterally arranged, with the paracortical cells always on the inside (or concave) half of the fibre curvature, led to the theory that it is the relative proportion and distribution of the orthocortex and paracortex patches that underpins intrinsic single-fibre curvature (Fraser and Rogers, 1954; Horio and Kondo, 1953). The theory has some experimental support from light- and electron-microscopy studies measuring average cell type distribution against average single-fibre curvature (Orwin et al., 1984; Snyman, 1963). The theory explains that, during keratinisation in the wool follicle, a fibre goes from a wet to a dry state, and that this affects the macrofibrils making up the cells of each cell type differently. Due to a greater number of intermediate filaments (IFs) in orthocortical macrofibrils that are initially tilted away from the fibre axis, longitudinal extension occurs during drying, and this extension in the orthocortex is believed to exceed that of paracortex, which is composed of macrofibrils in which the IFs are aligned along the fibre axis. The theory predicts that, in order to relieve internal strain

[1]Food and Bio-based Products Group, AgResearch, Lincoln 7608, New Zealand. [2]Hair Beauty Research, Kao Corporation, Tokyo 131-8501, Japan. [3]Farm Systems and Environment Group, AgResearch, Lincoln 7608, New Zealand.

*Authors for correspondence (duane.harland@agresearch.co.nz; Koike.kenzo@kao.co.jp)

D.P.H., 0000-0002-1204-054X; K.K., 0000-0002-6796-5785

Received 15 October 2017; Accepted 16 January 2018

Journal of Experimental Biology (2018) 221, jeb172312. doi:10.1242/jeb.172312

energies, the wool fibre will curl in the direction of the less-extended paracortical side (Brown and Onions, 1961; Dobozy, 1959; Munro and Carnaby, 1999). We refer to this theory as the 'cell type distribution model'.

The most convincing and well developed alternative theory is what we will call the 'cell proliferation model', and was established from observations of the relationship between follicle morphology and resultant fibre morphology (Auber, 1951). The proposed mechanism of the cell proliferation theory is that there is an asymmetry in the rate of cell division on either side of the follicle's dermal papilla. Consequently, the more prolific side of the follicle produces what will become the cortex closest to the outside (convex side) of the fibre's curvature. The cell proliferation model explains both intrinsic fibre curvature and the observation that there is a possible association between fibre curvature and degree of follicle bending (Nay and Johnson, 1967). In the cell proliferation model, the cell types *per se* are not directly involved in defining intrinsic curvature; there is just more material on one side of the fibre than the other. More recently, an advanced version of this theory has been developed in which resultant curvature is a trade-off between asymmetric cell production and differential onset of keratinisation on either side of the fibre axis within the follicle (Hynd et al., 2009).

We directly tested the two models using confocal microscopy by measuring cell type proportions and cell numbers and lengths in small pieces of fibre (snippets) of known specific intrinsic curvature but no apparent torsion, and found that, although neither theory fully explains curl, the cell types play a critical role.

MATERIALS AND METHODS

Samples

Six adult female merino sheep were sampled from a research flock aged between 3 and 10 years (Table S1). Samples were collected in June 2011 (winter) from sheep housed on a commercial farm in North Canterbury, New Zealand that had been on the farm under uniform feed and environmental conditions for 6 months prior to sampling. All samples were taken from a small mid-side patch using electric animal clippers and cut within a few millimetres of the skin surface. Sheep housing and wool collection procedures complied fully with New Zealand law and were reviewed and approved (AE Application 12188) by the AgResearch Invermay Animal Ethics Committee.

Sample cleaning, relaxation to intrinsic curvature and selection

Staples of wool were cleaned with heptane, ethanol and ethoxylated nonylphenol (Teric GN9) (0.15% in 60°C), and rinsed in ultrapure water. Two-thirds of each staple closest to the tip was then cut away and discarded. Individual fibres were removed by handling with fine forceps at their tip end only and attached by the root end to a strip of double-sided tape along one edge of a microscope slide. Only fibres in good condition with a regular appearance were selected. Each fibre was then cut down further so that only 20 mm closest to the root was retained, tethered at one end to the slide. Slides of fibres were submerged for 18 h in 500 ml of degassed ultrapure water containing 400 µl of 0.15% Teric GN9 (to disrupt surface tension bubbles on fibre surfaces). Individual fibres were removed by breaking them with forceps where they were attached to the tape, transferred to a dry sheet of cardboard surface on the baseplate of a high-vibration shaker (Retsch AS200; Retsch, Germany) and air dried at ambient conditions (20°C, 50% relative humidity) at a frequency and amplitude that kept the fibre mobile on the surface for 60 s. Fibres were stored in small Petri dishes until further cutting into snippets. Snippets were cut under a magnifier with dark-field illumination on a clean ceramic surface with a GEM single-edge razor blade. Individual snippets that had uniform curvature and no torsion were transferred, using static adhesion, onto a microscope slide. Using a dissecting microscope and transmitted light, snippets were carefully anchored at one end into a thin line of chemically inert acetic cure silicone cement (Selleys Glass Silicone Sealant; Selley's Ltd, Australia) to lie flat on the glass surface. Silicone cement was cured for at least 72 h at room temperature before any further processing. Each snippet was examined using a stereo light microscope, and those that were not lying flat against the slide and those in which curvature had become non-uniform were marked and not used in the study (about 50%). A total of 717 snippets were mounted and five from each sheep were selected for imaging. With no previous guide as to appropriate sample size, we chose a manageable target of 30–50 fibres for each experiment, and concentrated on selecting snippets with most uniform curvature and least torsion, thereby reducing two major potential sources of measurement error.

Measurement of intrinsic curvature

Slides were first dried over dry silica gel under a low vacuum for 24 h (measured 5–9% relative humidity) then immediately scanned dry at 2400 dpi in an Epson 3200 flatbed scanner (Fig. 1A). Measurements (deg mm^{-1}) were made from scans by fitting a circle to the region of curvature later used for confocal measurements (AnalySIS Five software; Olympus Imaging Systems, Germany). Curvature measurements were made only after confocal imaging so that the precise region of the snippet from which data were obtained could be identified. Following scanning, slides were stored under vacuum in the dark at room temperature until staining.

Staining for microscopy

Two sets of slides were produced for each sheep. One was stained to highlight orthocortical and paracortical differences, and the other stained to highlight cell boundaries.

For cell-type staining, we used an *en bloc* modification of the approach used in Bryson et al. (2009). Slides were placed in a staining trough, covered with a solution of 0.002% fluorescein sodium in 4% benzyl alcohol and left in the dark at 45°C for 18 h with gentle rocking. Fluorescein was drained off and slides washed briefly (30 s) twice in ultrapure water and then once in 4% benzyl alcohol before being immersed in a solution of 0.0005% sulforhodamine 101 in 4% benzyl alcohol in a staining trough and left for 1.5 h at 45°C in the dark. Finally, the stain was drained off the slides and they were washed briefly (30 s) three times in ultrapure water, blotted gently with tissue, dried carefully with compressed air from a can and stored under low-vacuum over dry silica gel in darkness.

For cell boundary staining, we followed a method reported by Sideris et al. (1990). Slides were sealed in an upright Coplin jar with a screw-top lid covered in a solution of 0.2 mg ml^{-1} rhodamine B in 9:1 ethanol:methanol for 18 h at 60°C. Slides were then rinsed for 20 s in perchloroethylene and dried in the dark for 30 min under a stream of nitrogen gas (Fig. S2). Slides were stored under low-vacuum over dry silica gel in darkness until use.

Confocal imaging and analysis

Slides were cover slipped with Dako anti-fade mounting medium and imaged using a laser scanning confocal microscope (Leica TCS SP5; Leica Microsystems, Wetzlar, Germany). Fibre snippets

Journal of Experimental Biology (2018) 221, jeb172312. doi:10.1242/jeb.172312

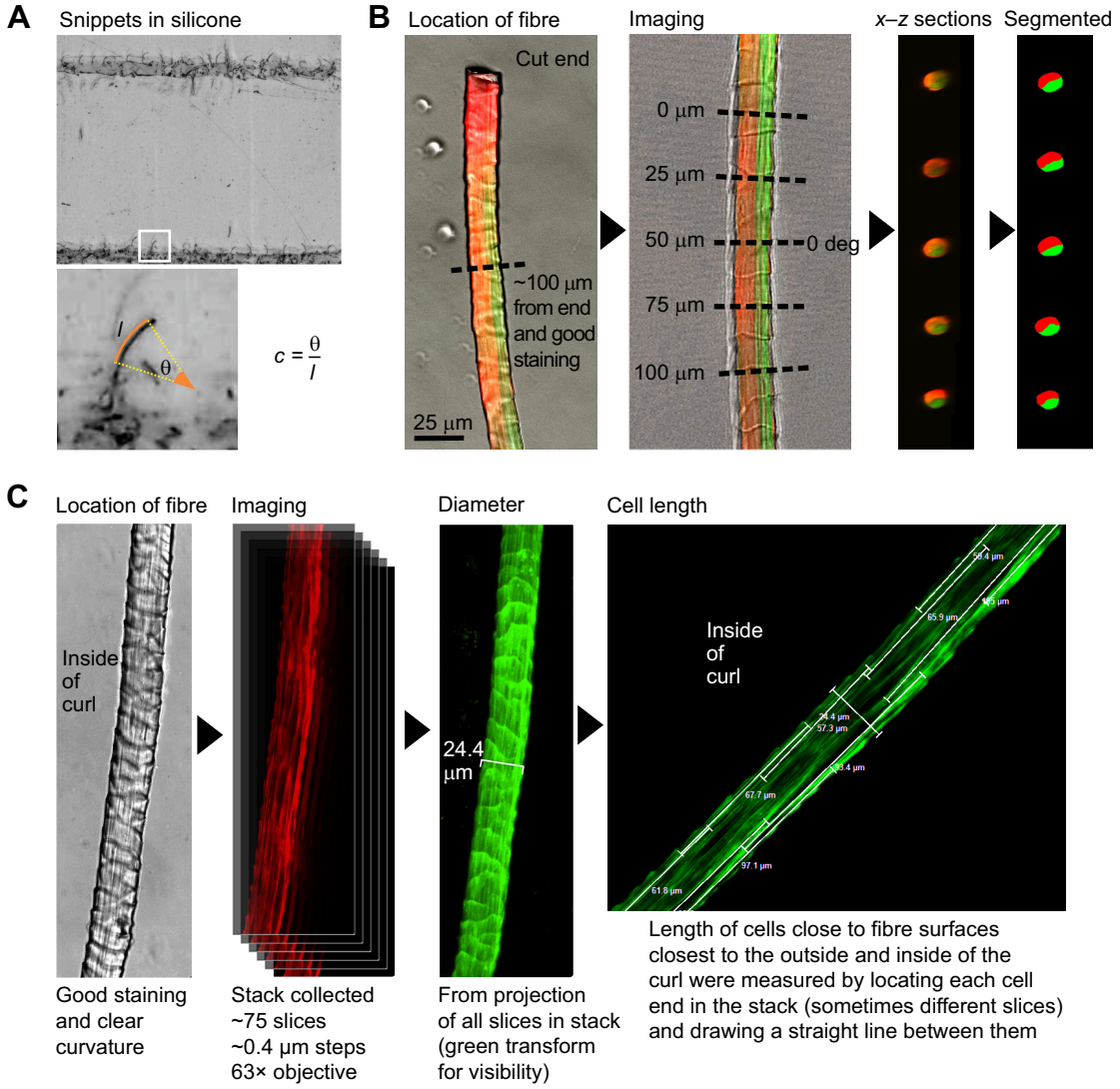

Fig. 1. Summary of methods used to collect data from wool snippets of uniform curvature. (A) Relaxed fibres cut into snippets were mounted in lines on microscope slides tethered by silicone. Curvature (*c*) of snippets was calculated from fitted arcs by dividing subtended angles (θ) by arc length (*l*). (B) Cell type imaging method from confocal virtual sections through the fibre. (C) Cell boundary imaging and cell length measurement from confocal stacks.

previously selected for imaging were located in bright field mode and then examined using laser confocal mode.

For cell type imaging, excitation wavelengths were tuned to the 488 and 561 nm laser lines (argon laser) for fluorescein and sulforhodamine, respectively. Snippets were first oriented and centred at a point >100 µm from the cut end and where staining was well defined. Then *x–z* images (optical cross-sections) were made directly at regular 25 µm intervals until a span of 100 µm had been covered. The orientation of the sample was periodically checked and adjusted so that each *x–z* section was transverse to the fibre longitudinal axis. Each *x–z* image from each snippet was enhanced by adjusting brightness and contrast. Fibre perimeter was manually traced and the same process was used for images of each cell type to segment the orthocortical and paracortical regions into red and green, respectively (Fig. 1B). Measurements of orthocortical and paracortical regions were made using automatic image analysis tools (AnalySIS Five) (Fig. S3).

For cell boundary samples, a Leica 63× glycerol immersion objective (HCX PL APO 1.30NA) with laser tuned to sulforhodamine excitation spectrum was used to collect stacks through selected snippets at a point of uniform curvature. Measurements of cell length were made from Leica's LAS AF software (V 2.6 2011; Leica Microsystems, Wetzlar, Germany) directly from stacks. Fibre diameter was measured from the projected image of all slices of the stack combined into a single image and is the diameter across the fibre's plane of curvature.

Cell length was measured by identifying the location of cell ends by moving through the image stack and by changing image brightness/contrast. A straight line was then drawn between cell ends (Fig. 1C). It was possible to measure cell lengths and edges throughout the width of the fibre, but we chose to only measure cells within two full cell widths of the fibre cuticle (Fig. S4). In preliminary studies, we established that this ensured that those cells measured on the outside of the curvature were always orthocortex type and those on the inside always paracortex type, and avoided any subjective bias that might have arisen from trying to discriminate cell type based on faint differences in stain colour and intensity.

To examine the hypothesis that curvature is caused by higher numbers of cells end-on-end along the side of the fibre on the

Journal of Experimental Biology (2018) 221, jeb172312. doi:10.1242/jeb.172312

outside of curvature, it was necessary develop a metric to enable sample-to-sample comparison measured in a number of cells per unit fibre length. This was difficult because the number of cells end-to-end along one or the other side of the fibre could not easily be directly measured by counting. There were multiple reasons for this: (1) the staining in many fibres did not clearly indicate the edges of every cell; (2) cells were often tilted or not straight; and (3) the outer surfaces of the fibre were often lumpy.

Our solution was to calculate the number of cells on the inside and the outside of the curvature based on geometric data that we could collect accurately from each sample (Fig. 2). Our calculation of cells/length was based on the assumption that the average percentage overlap for neighbouring cells was similar in both the orthocortex and paracortex, something that is supported by earlier transmission electron microscopy (TEM) and current confocal observations. We based our calculation on a 250 µm length of fibre because this was a similar scale to the region over which cell lengths were measured.

Statistical software and data availability

All statistical analyses were carried out on GraphPad Prism V4.03 (San Diego, CA, USA). Measurement data are available in online repository figshare (https://doi.org/10.6084/m9.figshare.5500873.v1).

RESULTS

Cell type measurements

In all cases, cell type regions were clearly differentiated in fibre cross-sections, cell type regions were bilaterally distributed, the paracortex was always within the half of the cortex closest to the inside of the fibre curvature, and the orthocortex was predominantly within the cortex half closest to the outside of the curvature.

The selected snippets (n=5 each from 6 sheep) covered a wide range of diameters and curvatures, and there was a negative trend between curvature and diameter (Fig. S5, dataset 1).

With the exception of one snippet, the orthocortical cell region always had a greater cross-sectional area than the paracortex. Over the range of curvatures in this study, the cross-sectional areas of both the orthocortical and paracortical regions increased with increasing fibre diameter (Fig. 3A). However, there appeared to be no clear relationship between curvature and the area of each cell type (Fig. 3B) (Table S2, datasets 2 and 3).

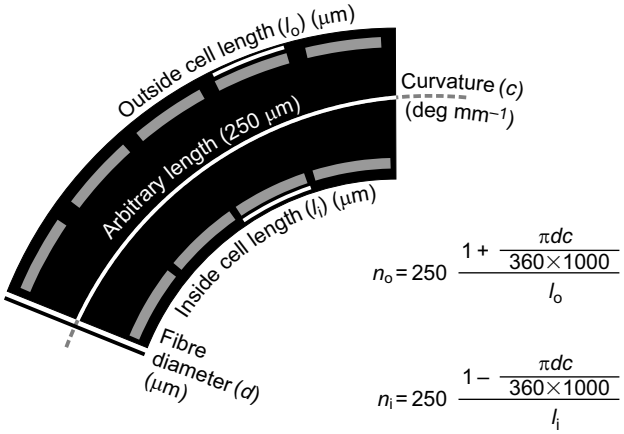

Fig. 2. Calculation of cell number in relation to fibre snippet diameter and curvature. n_o and n_i are the number of end-on-end cells along the outside and inside edges, respectively, of 250 µm of fibre with diameter d and curvature c, based on average length measurements for cells along the outside (l_o) and inside (l_i), respectively.

We considered that it may not be the cell type alone that may relate to curvature but other measures relating to the proportion of cell types. However, none of the following measures appeared to correlate with curvature (Table S2): individual proportion within a snippet (Fig. 4A); the net difference between the two types as a proportion of the overall diameter of the snippet (Fig. 4B); or the distance between the central points (centre of mass/gravity) of each cell type region (Fig. 4C,D).

All virtual (x–z) sections of all snippets in this study were bilaterally symmetric and divided into single orthocortical and paracortical patches. We investigated whether the shape of the patches (as opposed to the size) related to fibre curvature. In transverse section, the region of paracortex was typically observed to be semi-circular or elliptical. In the case of a paracortical region of elliptical shape, 'arms' of orthocortex wrapped partly around the paracortex close to the cuticle at its narrow ends. We considered that the placement of orthocortical material alongside paracortical material close to the cuticle on the inside curve side of the cortex could potentially influence snippet curvature. We studied this possible effect by measuring orthocortical convexity (the difference between the area of the shape's convex hull and its actual area, i.e. a measure of how convoluted a shape's profile is) (Fig. S2) and comparing it with curvature (Fig. 5A), but found no relationship (Table S2). In addition, we examined the aspect ratio (Fig. 5B) and the circularity (a measure of roundness, where a perfect circle=1) of the regions (Fig. 5C), but found no correspondence between shape of cell type regions and curvature.

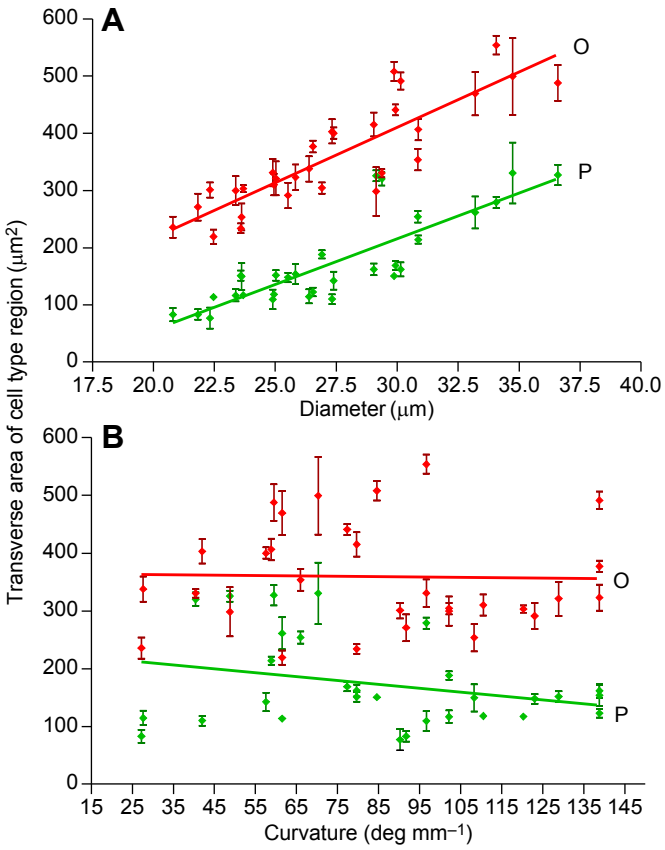

Fig. 3. Area of orthocortical and paracortical regions. Cross-sectional areas of orthocortical (O; red) and paracortical (P; green) regions plotted against (A) snippet diameter and (B) snippet curvature. Points are means±s.e.m. of 5 locations along each of 30 snippets (6 from 5 sheep). Lines (A,B) are linear regressions.

Journal of Experimental Biology (2018) 221, jeb172312. doi:10.1242/jeb.172312

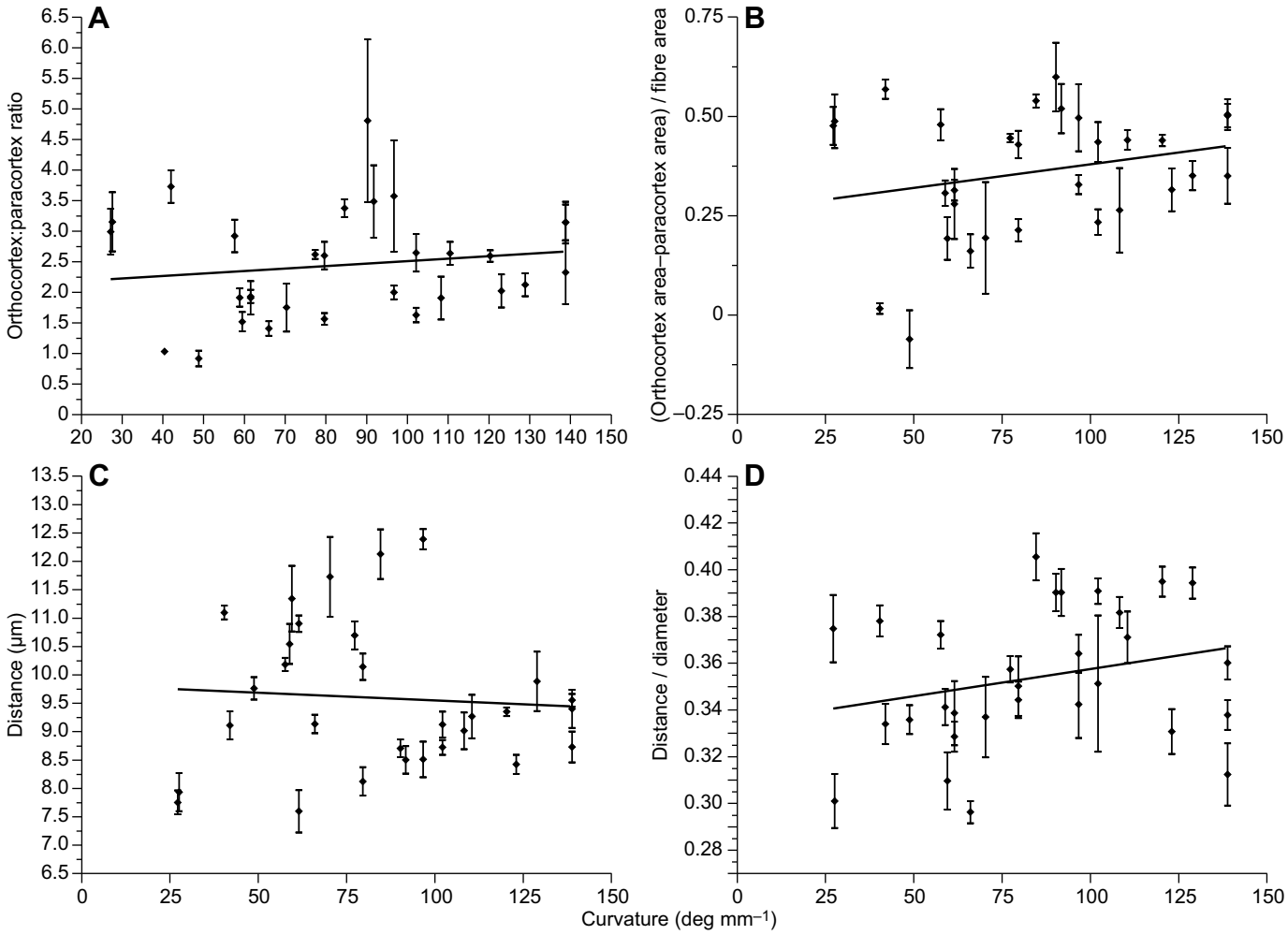

Fig. 4. Relative differences between cell types plotted against curvature in wool snippets. (A) Ratio of orthocortical to paracortical area. (B) Difference between the cross-sectional area of orthocortex and paracortex as a proportion of snippet cross-section area. (C) Distance between central points of orthocortical and paracortical area. (D) Distance between central points normalised by diameter of snippet. Points are means±s.e.m. of 5 locations along each of 30 snippets (6 from 5 sheep). Lines (A–D) result from linear regressions.

Cell length/number measurements

In all stacks of snippets stained for cell boundaries, we were able to use difference in the intensity of staining across the fibre to differentiate between orthocortex and paracortex. This allowed us to confirm that all samples had cell types that were bilaterally distributed and that the paracortex was always within the half of the cortex closest to the inside of the fibre curvature. The selected snippets (n=5 each from 6 sheep and an additional n=10 each from 2 sheep) covered a wide range of diameters and curvatures (Fig. S6A) and were highly variable between different snippets from single sheep. Again, the relationship between diameter and curvature was found to be noisy (Fig. S6B) but negatively correlated (Table S3).

Measurements of cell length resulted in a sizable data set (n=344 cells) across the 50 wool snippets. The data from the inside and outside of the curve (Fig. 6A) were normally distributed (Kolmogorov–Smirnov test), and cells from close to the inside of the curl were significantly shorter than cells close to the outer side (unpaired two-tailed t-test, P<0.0001, t=12.84, d.f.=342).

The two distributions of cell lengths had considerable overlap (Fig. 6B). A key finding here is that in every fibre we examined the average length of orthocortical cells for that fibre was longer than that of paracortical cells from the same fibre. This is clearly seen when the data are plotted as pairs (Fig. 6C).

We observed that the average length of cells measured for a single fibre increased with fibre diameter irrespective of position with respect to curvature (Fig. 7A) (Table S3). Against curvature, only the paracortical cells showed a statistically significant relationship, in which higher curvature was associated with shorter paracortical cells (Fig. 7B). The difference in cell length (outside minus inside length) for each snippet increased with increasing fibre curvature (Fig. 7C), and this was also the case when the data were normalised against fibre diameter (Fig. 7D).

We estimated the number of cells along 250 μm of fibre along the inside and the outside of each fibre by combining data on the curvature, diameter and cell length measurements from each snippet (see Fig. 2). From these data we determined the ratio of cell numbers on each side of the fibres and analysed this with respect to fibre diameter (Fig. 8A) and curvature (Fig. 8B). Both results indicate that there are generally more cells on the inside of curvature of a fibre despite the shorter arc length on the inside of a curved fibre. Although increases in diameter do not appear to affect this relationship, increasing fibre curvature appears to increase the relative difference in cell numbers on the two sides of the fibre

Journal of Experimental Biology (2018) 221, jeb172312. doi:10.1242/jeb.172312

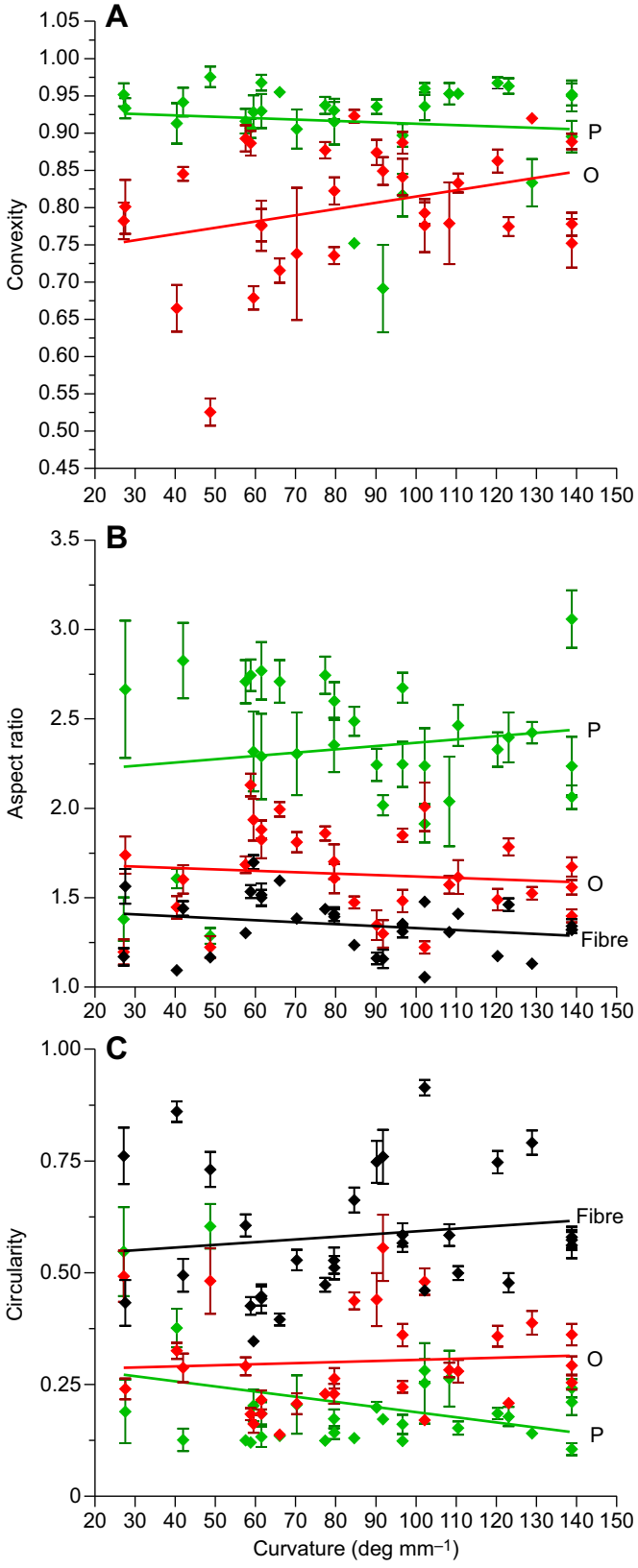

Fig. 5. Analysis of shape factors. (A) Convexity (complexity of shape) of the orthocortical (O; red) and paracortical (P; green) regions from snippet cross-sections plotted against snippet curvature. Lower convexity scores typically indicate that the orthocortex partially surrounds the paracortex. (B) Aspect ratio (measure of elongation) of each cell type region. (C) Circularity. Points are means±s.e.m. of 5 locations along each of 30 snippets (6 from 5 sheep). Lines are linear regressions.

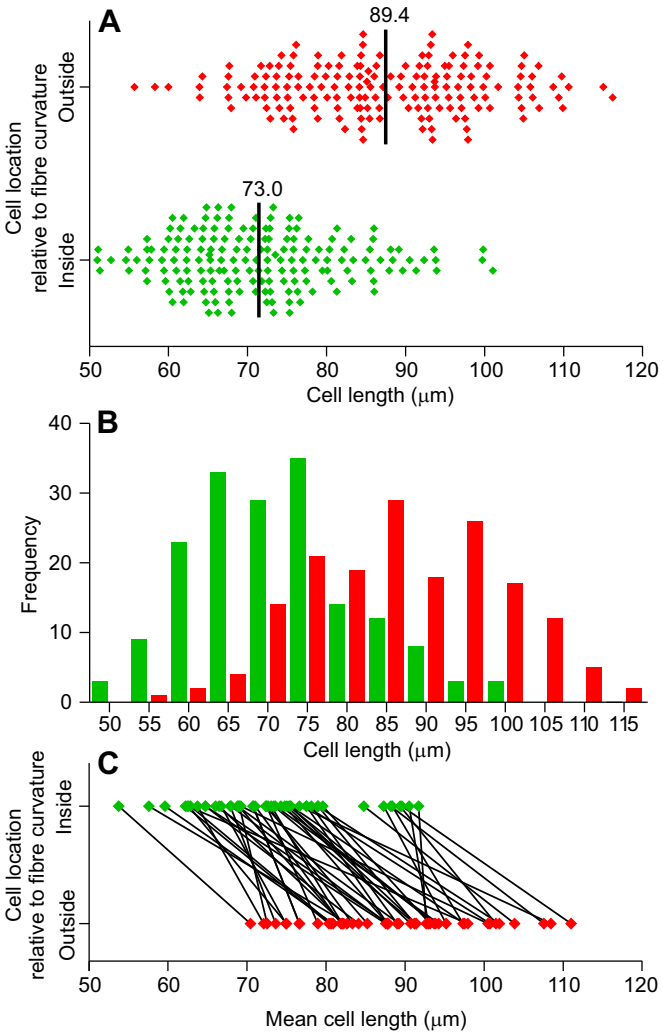

Fig. 6. Cell length differences between the inside and outside of snippet curvatures. Inside (paracortex; green); outside (orthocortex; red). (A) Distribution of cell lengths from all cells (n=344, 50 snippets). Cells from close to the inside of the curl were significantly shorter than cells close to the outer side (unpaired two-tailed t-test, P<0.0001, t=12.84, d.f.=342). (B) Frequency distribution showing overlap between cell length distributions. (C) Paired plot of mean lengths. Each pair from a single snippet is connected by a line. In all cases lines have a negative slope, indicating that, for each snippet, cells close to the outside of the curl are longer than those close to the inside of curl.

(Table S3). It is, however, a weak statistical relationship and may be associated with the tendency for cells on the inside of the fibre curvature to become shorter with increasing curvature (Fig. 7B).

DISCUSSION

Our *in situ* measurements of cell types and cell lengths for regions in which the curvature at the point of measurement was also measured allowed us to directly test current theories of fibre curvature, which were built on indirect data. However, it should be noted that the 3D shape of a single fibre is generally a product of fibre curvature and torsion. Our findings are focused explicitly on the curvature component of single-fibre shape.

One of the current models of fibre curvature, the cell type distribution model, proposes that curvature is caused by the relative amount and distribution of orthocortical and paracortical cells, because orthocortical cells will be uniformly longer than paracortical cells. The hypothesis is that this length difference is

Journal of Experimental Biology (2018) 221, jeb172312. doi:10.1242/jeb.172312

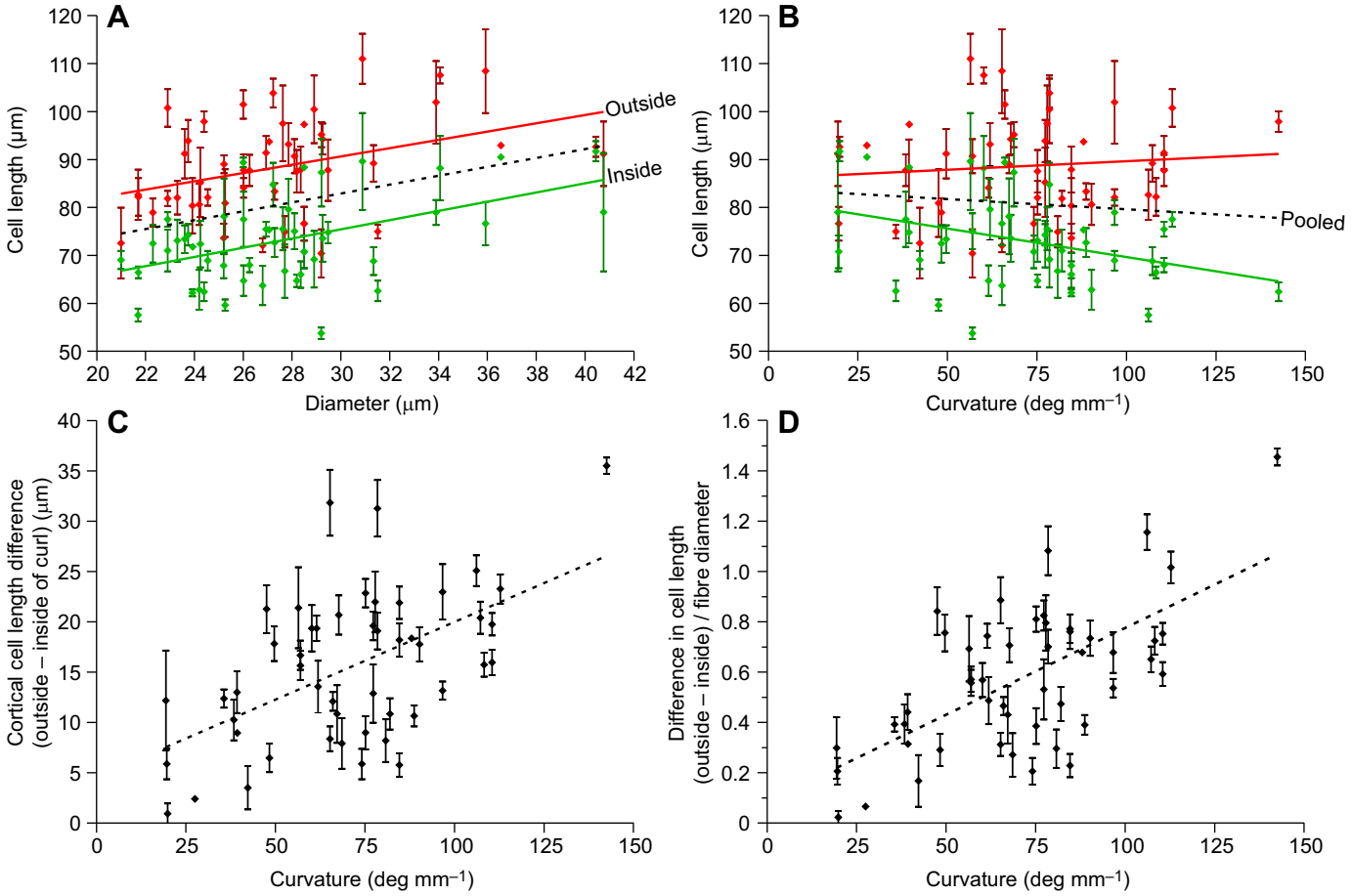

Fig. 7. Cell length analysis. (A) Length of both cell types increased with fibre diameter. (B) High curvature was associated with shorter paracortical cells (green), whereas orthocortical cell lengths (red) were not particularly related to curvature. (C) The difference in average cell length (outside to inside) increased significantly with increasing curvature (linear regression, r^2=0.3, deviation from 0 P<0.0001) and, (D) also when normalised by fibre diameter (linear regression, r^2=0.42, deviation from 0 P<0.0001). Points are means±s.e.m. of cells measured from 50 snippets (n=5 each from 6 sheep and an additional n=10 each from 2 sheep). Lines are linear regressions. Green points are data from cells on the inside of the curvature and red for data from cells on the outside of curvature. Black lines are for pooled data.

caused by orthocortical extension, as predicted by Munro and Carnaby (1999); their work used mathematical modelling to predict how macrofibrils with differently arranged intermediate filaments would change in length because of the drying and shrinkage that occurs during fibre hardening. Munro and Carnaby concluded that macrofibrils with a double-twist arrangement, typical of orthocortical cells, should extend significantly more due to lateral shrinkage than macrofibrils with filaments arranged in parallel, typical of paracortical cells. Microbeam small angle X-ray studies have shown that average intermediate filament angle increases on the outside of curvature of both merino wool (Kajiura et al., 2005) and in the much higher diameter curly human scalp hair from a range of ethnic origins (Kajiura et al., 2006), suggesting that average macrofibril double-twist intensity (Harland et al., 2014) varies across the cortex in a way that is consistent with longer cells on the outside of the curvature.

Our data strongly support this model, but with some key additions. As it stands, the cell distribution model assumes that all orthocortical cells have a similar distribution of length irrespective of fibre or animal, and that the same is true for paracortical cells. This assumed universal difference in cell type length is what should allow curvature to be predicted from proportions and distributions of the cell types within the model (Liu and Bryson, 2002). We would expect this relationship to be particularly clear in fibres that have the combination of especially high curvature, clearly differentiated cell types and simple cell type distributions, such as in merino wool. Although orthocortical cells were significantly longer than paracortical cells (Fig. 6A,B) when averaged across fibres and animals, we found no evidence to support the assumed universal link between the relative amount of each cell type and curvature (Fig. 4). Our data indicate that cell length differences between orthocortical and paracortical cells that correlate with curvature are location specific. That is, two hairs that have the same sized patches of paracortex and orthocortex could have different curvatures because the fibres differ in the relative length of their orthocortical and paracortical cells.

Our results were obtained from merino fibres that had low diameter and high curvature, cell types that were clearly differentiated into orthocortex and paracortex, and that showed clear bilateral symmetry in their distribution. Further study will be required to establish how this variation between fibres and animals extrapolates to fibres with less differentiated morphology. In particular, the relationship between curvature, diameter and cell length will require investigation in fibres with higher diameters. For example, it is possible that variation in cell type length may decrease with increasing diameter, leading to some fibres in which the proportion of cell types does correlate with curvature – higher

Journal of Experimental Biology (2018) 221, jeb172312. doi:10.1242/jeb.172312

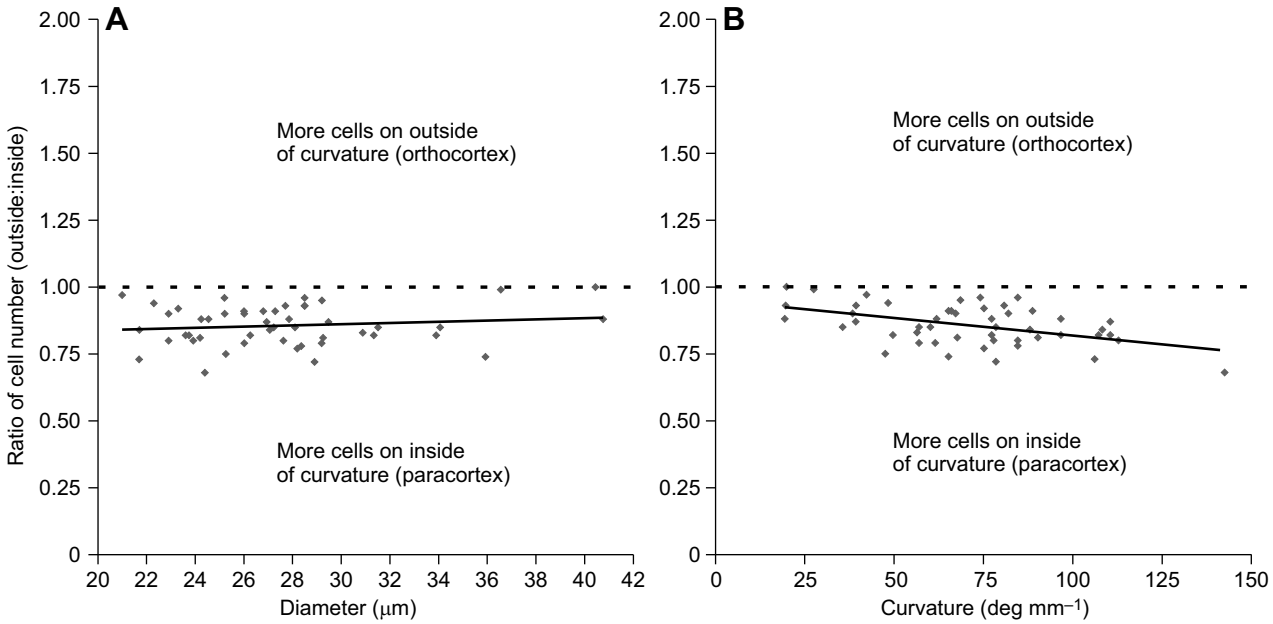

Fig. 8. Ratio of number of cortical cells on the outside and inside of curvature. Data are from 50 snippets (n=5 each from 6 sheep and an additional n=10 each from 2 sheep). (A) No apparent relationship exists with fibre diameter. The dashed line indicates the point at which there are the same numbers of cells on the inside and on the outside curvature of the fibre and points below that line indicate fibres in which there are more cells along the inside curve of the fibre. (B) A significant negative relationship was found with curvature.

diameter fibres such as human scalp hairs appear to have cell types that are less clearly differentiated than those found in merino wool (Bryson et al., 2009; Harland et al., 2014).

Further study will also be required to understand the mechanism that controls cell length in developing fibres. Two factors in particular that may affect cell length are the process of cell reshaping and ordering that occurs in the elongation region of the follicle (Orwin and Woods, 1982), and differences in the proportions of macrofibrils with increased double-twist intensity (related to the average helical tilt of the intermediate filaments) within and between cortical cells (Harland et al., 2011, 2014). The two factors are not mutually exclusive, and may also be underpinned by differential protein expression across the bulb (Thibaut et al., 2007) and associated differences in the macrofibril self-assembly processes (McKinnon and Harland, 2011).

Another theory of fibre curvature, which we term the cell proliferation model, explains fibre curvature as a product of differential cell division rates in follicles that results in the side of the fibre on the outside of the curvature having more cells than the inner side (Auber, 1951; Hynd et al., 2009). We found no evidence in the current study that supports this theory, although we recognise that our cell number data are derived from a calculation of cell numbers and not a direct count, and the precision of the data is less than if we were able to count the cells directly. However, there were never more cells on the outside of curve than the inside because the ratio of cells outside:inside was one or less in every fibre (Fig. 8).

Our study measured the length of cortical cells *in situ*, and the data indicate an average cell length of 73.0 μm for paracortical cells and 89.4 μm for orthocortical cells (Fig. 6). Cortical cells have traditionally been assumed to be of slightly variable dimensions but approximately 100 μm long and 5 μm wide irrespective of cell type (Hynd, 1994; Orwin, 1979). Our results complement earlier TEM studies of merino wool cross-sections, which concluded that orthocortical cells are larger than paracortical cells (Bones and Sikorski, 1967; Kassenbeck and Leveau, 1957; Orwin et al., 1984) based on TEM measurements of the maximum width of cortical cells. Our own unpublished TEM study on 21 μm merino fibres (Harland et al., 2006) also found that orthocortical cells had a significantly higher diameter (mean minimum=3.16 μm, mean maximum=5.89 μm; n=605) than did paracortical cells (mean minimum=2.46 μm, mean maximum=4.56 μm; n=557). The confocal data presented here add to this conclusion by indicating that, irrespective of cell type, cortical cells that are wider are also longer.

The few studies to investigate merino fibre cortical cell length have relied on measuring cells that have been enzymatically or chemo/mechanically isolated, usually dried and typically measured using scanning electron microscopy. Historic measurements include (length×maximum width): 95×5.5 μm (Lockhart, 1960); 102×3.6 μm (Kulkarni et al., 1971); and 109×5.2 μm from our own

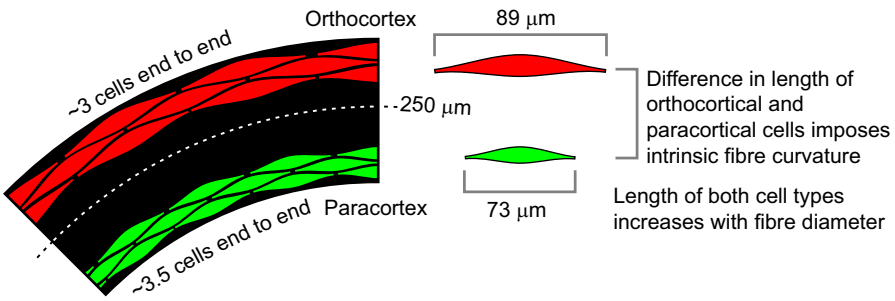

Fig. 9. Summary of findings concerning a model of intrinsic fibre curvature caused by the difference in orthocortical and paracortical cell length. Absolute length of each cell type varies from location to location, but the relative difference in length of the two cell types underpins curvature.

unpublished studies on 300 merino fibres with average diameter of 21 µm (Harland et al., 2006). This raises the question of why cells measured in this study were considerably shorter than in these earlier studies. One possible reason is that we were not measuring from the same points as for isolated cells because the packing of fibres *in situ* may constrain them. Also, our *in situ* cells were in fibres immersed in an anti-fade compound, which probably contains water, which may reduce the length of orthocortical cells due to swelling.

Conclusion: a revised model of intrinsic curvature in hairs

Our data led us to hypothesize that intrinsic fibre curvature at a specific location in merino wool fibres is a function of the relative difference in length between orthocortical and paracortical cells on the outside and inside, respectively, of the cortex along the plane of curvature. What we propose is a modified version of the cell type distribution model (Fig. 9). The relative difference is dynamic because cell length varies between fibres and possibly also along fibres. We hypothesize that intrinsic cortical cell length is controlled by processes in the follicle (including cell shaping), the inclusion of double-twist macrofibrils (i.e. similar to those in the orthocortex) within paracortical cells, or through variation in macrofibril double-twist intensity (see McKinnon and Harland, 2011). Intrinsic curvature is then modified by extrinsic factors such as dry set, disulfide exchange or the introduction of other crosslinks to result in a final curvature. This curvature contributes to the overall 3D shape of a fibre, which is a product of curvature and torsion. We believe that the inclusion of variation in cortical cell length as a parameter of the mechanism underpinning curvature should be universally applicable to mammalian keratin hairs.

Acknowledgements

We thank Manfred Ingerfeld and David Collings from the School of Biological Sciences and Biomolecular Interaction Centre, University of Canterbury, for assistance with confocal microscopy. We are also grateful for technical assistance and advice during the course of the research from Erin Lee, Ancy Thomas, Denis O'Connell and Chikako van Koten.

Competing interests

The authors declare no competing or financial interests.

Author contributions

Conceptualization: D.P.H., J.L.W., S.N., T.I., K.K.; Methodology: D.P.H., J.A.V., J.L.W.; Validation: J.L.W.; Formal analysis: D.P.H.; Investigation: D.P.H., J.A.V., J.L.W.; Resources: D.A.S., A.J.G.; Data curation: J.A.V.; Writing - original draft: D.P.H., J.L.W.; Writing - review & editing: J.A.V., J.L.W., S.N., T.I., K.K., D.A.S., A.J.G., J.M.D., S.C.; Supervision: T.I., K.K., J.M.D., S.C.; Project administration: J.M.D., S.C.; Funding acquisition: S.N., T.I., K.K.

Funding

This work was supported by Kao Corporation and by AgResearch through its Integrated Wool Sciences Programme (New Zealand Government Ministry of Business Innovation & Employment, Science strategic investment fund).

Data availability

Measurement data are available from figshare (https://doi.org/10.6084/m9.figshare.5500873.v1).

Supplementary information

Supplementary information available online at
http://jeb.biologists.org/lookup/doi/10.1242/jeb.172312.supplemental

References

Alibardi, L. (2006). Structural and immunocytochemical characterization of keratinization in vertebrate epidermis and epidermal derivatives. *Int. Rev. Cytol.* **253**, 177-259.

Auber, L. (1951). The anatomy of follicles producing wool-fibres, with special reference to keratinization. *Trans. Roy. Soc. Edin.* **62**, 191-254.

Bonès, R. M. and Sikorski, J. (1967). The histological structure of wool fibres and their plasticity. *J. Text. Inst.* **58**, 521-532.

Brown, T. D. and Onions, W. J. (1961). A theory for the development of wool fibre crimp on drying. *J. Text. Inst.* **52**, 101-109.

Brunner, H. and Coman, B. J. (1974). *The Identification of Mammalian Hair*, 1st edn. Melbourne: Inkata Press.

Bryson, W. G., Harland, D. P., Caldwell, J. P., Vernon, J. A., Walls, R. J., Woods, J. L., Nagase, S., Itou, T. and Koike, K. (2009). Cortical cell types and intermediate filament arrangements correlate with fiber curvature in Japanese human hair. *J. Struct. Biol.* **166**, 46-58.

Dobozy, O. K. (1959). The shape and cause of wool crimp. *Text. Res. J.* **29**, 836-839.

Fish, V. E., Mahar, T. J. and Crook, B. J. (1999). Fibre curvature morphometry and measurement. *Wool Tech. Sheep Breed.* **47**, 248-265.

Fraser, R. D. B. and Rogers, G. E. (1954). The origin of segmentation in wool. *Biochem. Biophys. Res. Commun.* **13**, 297-298.

Harland, D. P., Caldwell, J. P., Walls, R. J., Woods, J. L., Vernon, J. A., Bryson, W. G., Liu, H. and Krsinic, G. L. (2006). *Australian Merino Wool Structural Database*. Lincoln, New Zealand: Australian Wool Innovation Limited.

Harland, D. P., Caldwell, J. P., Woods, J. L., Walls, R. J. and Bryson, W. G. (2011). Arrangement of trichokeratin intermediate filaments and matrix in the cortex of merino wool. *J. Struct. Biol.* **173**, 29-37.

Harland, D. P., Walls, R. J., Vernon, J. A., Dyer, J. M., Woods, J. L. and Bell, F. (2014). Three-dimensional architecture of macrofibrils in the human scalp hair cortex. *J. Struct. Biol.* **185**, 397-404.

Harland, D. P., Woods, J. L., Vernon, J. A., Walls, R. J., Scobie, D. R., Plowman, J. E., Cornellison, C., Craven, T., Itou, T., Koike, K. et al. (2015). Like follicle, like fibre? Diameter and not follicle type correlates with fibre ultrastructure. *Key Eng. Mater.* **671**, 88-94.

Horio, M. and Kondo, T. (1953). Crimping of wool fibers. *Text. Res. J.* **23**, 373-386.

Hynd, P. I. (1994). Follicular determinants of the length and diameter of wool fibres I. Comparison of sheep differing in fibre length/diameter ratio at two levels of nutrition. *Aust. J. Agr. Res.* **45**, 1137-1147.

Hynd, P. I., Edwards, N. M., Hebart, M., McDowall, M. and Clark, S. (2009). Wool fibre crimp is determined by mitotic asymmetry and position of final keratinisation and not ortho- and para-cortical cell segmentation. *Animal* **3**, 838-843.

Kajiura, Y., Watanabe, S., Itou, T., Iida, A., Shinohara, Y. and Amemiya, Y. (2005). Structural analysis of single wool fibre by scanning microbeam SAXS. *J. Appl. Crystalography* **38**, 420-425.

Kajiura, Y., Watanabe, S., Itou, T., Nakamura, K., Iida, A., Inoue, K., Yagi, N., Shinohara, Y. and Amemiya, Y. (2006). Structural analysis of human hair single fibres by scanning microbeam SAXS. *J. Struct. Biol.* **155**, 438-444.

Kassenbeck, P. and Leveau, M. (1957). Nouvelles methodes d'examen de coupes de fibres au microscope electronique application a l'etude de la structure de la laine. *Bulletin de l'institut Textile de France* **67**, 7-18.

Kulkarni, V. G., Robson, R. M. and Robson, A. (1971). Studies on the orthocortex and paracortex of Merino wool. *Appl. Polymer Symp.* **18**, 127-146.

Liu, H. and Bryson, W. G. (2002). A three-component model of the wool fibre - effects of morphology, elasticity and intermediate filament arrangement on fibre stiffness. *J. Text. Inst.* **93**, 121-131.

Lockhart, L. W. (1960). The size of cortical cells in wool fibres. *J. Text. Inst.* **51**, T295-T297.

Maderson, P. F. A. (2003). Mammalian skin evolution: A reevaluation. *Exp. Dermatol.* **12**, 233-236.

McKinnon, J. and Harland, D. P. (2011). A concerted polymerization-mesophase separation model for formation of trichocyte intermediate filaments and macrofibril templates 1: Relating phase separation to structural development. *J. Struct. Biol.* **173**, 229-240.

Munro, W. A. and Carnaby, G. A. (1999). Wool fibre crimp, Part I: the effects of micro-fibrillar geometry. *J. Text. Inst.* **90**.

Nay, T. and Johnson, H. (1967). Follicle curvature and crimp size in some selected Australian Merino groups. *Aust. J. Agr. Res.* **18**, 833-840.

Orwin, D. F. G. (1979). The cytology and cytochemistry of the wool follicle. *Int. Rev. Cytol.* **60**, 331-374.

Orwin, D. F. G. and Woods, J. L. (1982). Number changes and development potential of wool follicle cells in the early stages of fiber differentiation. *J. Ultrastructure. Res.* **80**, 312-322.

Orwin, D. F. G., Woods, J. L. and Ranford, S. L. (1984). Cortical cell types and their distribution in wool fibres. *Aust. J. Biol. Sci.* **37**, 237-255.

Ryder, M. L. (1964). Fleece evolution in domestic sheep. *Nature* **204**, 555-559.

Ryder, M. L. (1973). *Hair*, 1st edn. London: Edward Arnold.

Sideris, V., Holt, L. A. and Leaver, I. H. (1990). A microscopical study of the pathway for diffusion of rhodamine B and octadecylrhodamine B into wool fibres. *J. Soc. Dyers & Colourists* **106**, 131-135.

Snyman, J. G. (1963). Cortical bilateral structure and wool crimp. *Text. Res. J.* **33**, 803-809.

Thibaut, S., Barbarat, P., Leroy, F. and Bernard, B. A. (2007). Human hair keratin network and curvature. *Int. J. Derm.* **46**, 7-10.

Woods, J. L., Harland, D. P., Vernon, J. A., Krsinic, G. L. and Walls, R. J. (2011). Morphology and ultrastructure of antler velvet hair and body hair from red deer (*Cervus elaphus*). *J. Morph.* **272**, 34-49.

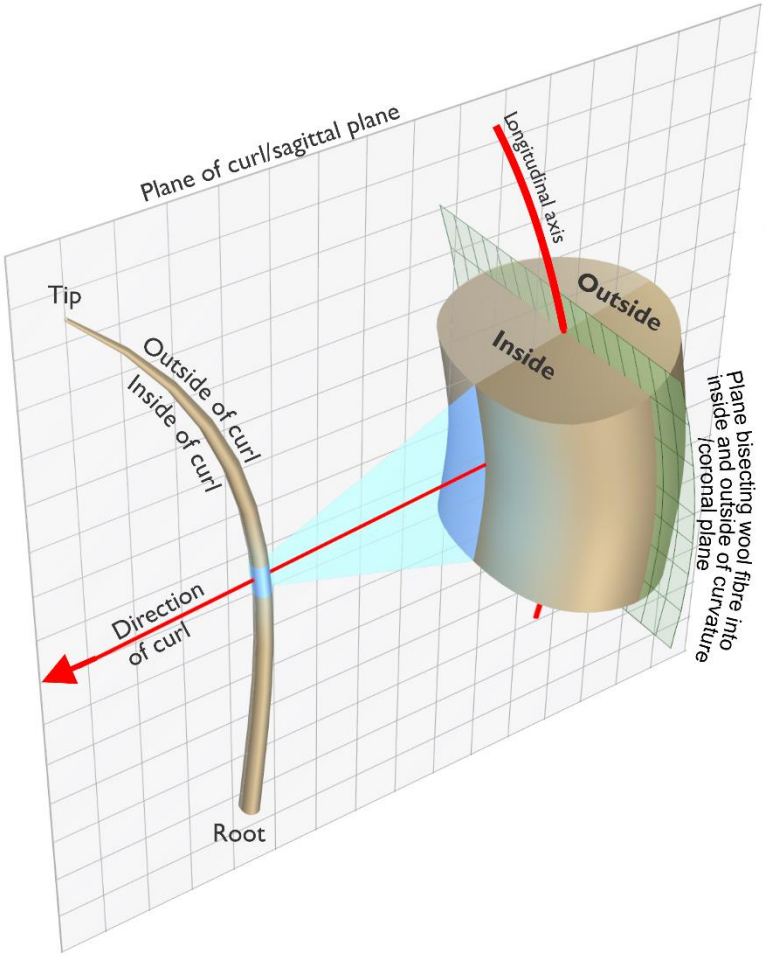

Fig. S1. Graphic definition of what is meant by inside, outside of curl and of fibre, and the direction of curl in main text.

Table S1. Sheep used in study. Body live weight measured before and after wool collection. Body condition score is an expert observer subjective score from (1 = emaciated to 5 = fat). Curvature and diameter are grand means of measurements for all snippets measured using methods described in text (fibres were chosen to maximise the range of curvatures for each sheep).

Tag	Body wt. (kg)		Body cond. score		Mean Curvature	Mean Diameter
	Apr	Oct	Apr	Oct	(SD) °/mm	(SD) µm
477	62.8	65.2	4	4	56.8 (27.1)	30.1 (3.7)
482	62.0	66.6	4	4	58.8 (28.5)	30.7 (6.0)
MR17	60.4	69.4	4	4	69.6 (23.1)	27.0 (3.0)
TB2	56.2	58.8	4	3	77.6 (30.8)	25.6 (2.5)
TA25	67.6	70.0	5	4	78.2 (19.0)	30.9 (5.0)
TB8	64.6	71.4	4	4	83.8 (30.9)	25.7 (2.7)
TB6	65.6	68.8	4	4	87.7 (36.9)	25.7 (2.6)
VL12	56.4	58.4	3	3	90.2 (28.0)	24.7 (2.5)

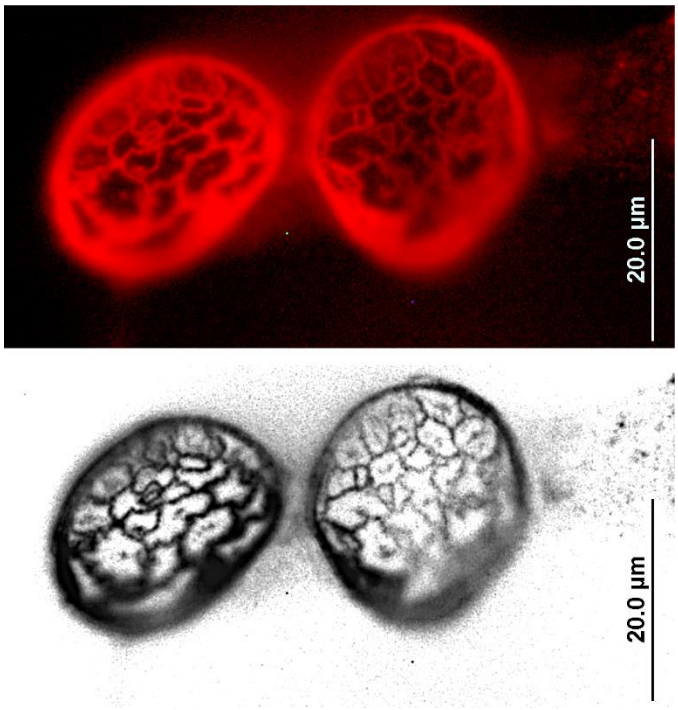

Fig. S2. Optical cross-sections from confocal microscopy of merino wool stained with cell boundary staining method taken during method development. The inverted and sharpened version in the bottom panel illustrates that cell boundaries are clearly visible throughout the fibre.

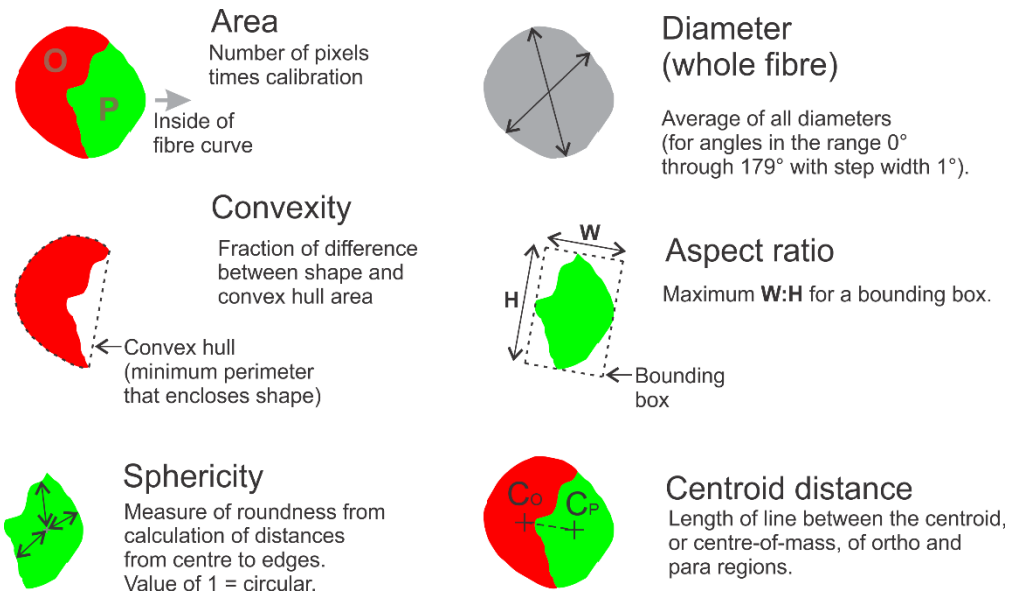

Fig. S3. Definitions of the key image analysis measurements made on segmented fibre images and fibre profiles.

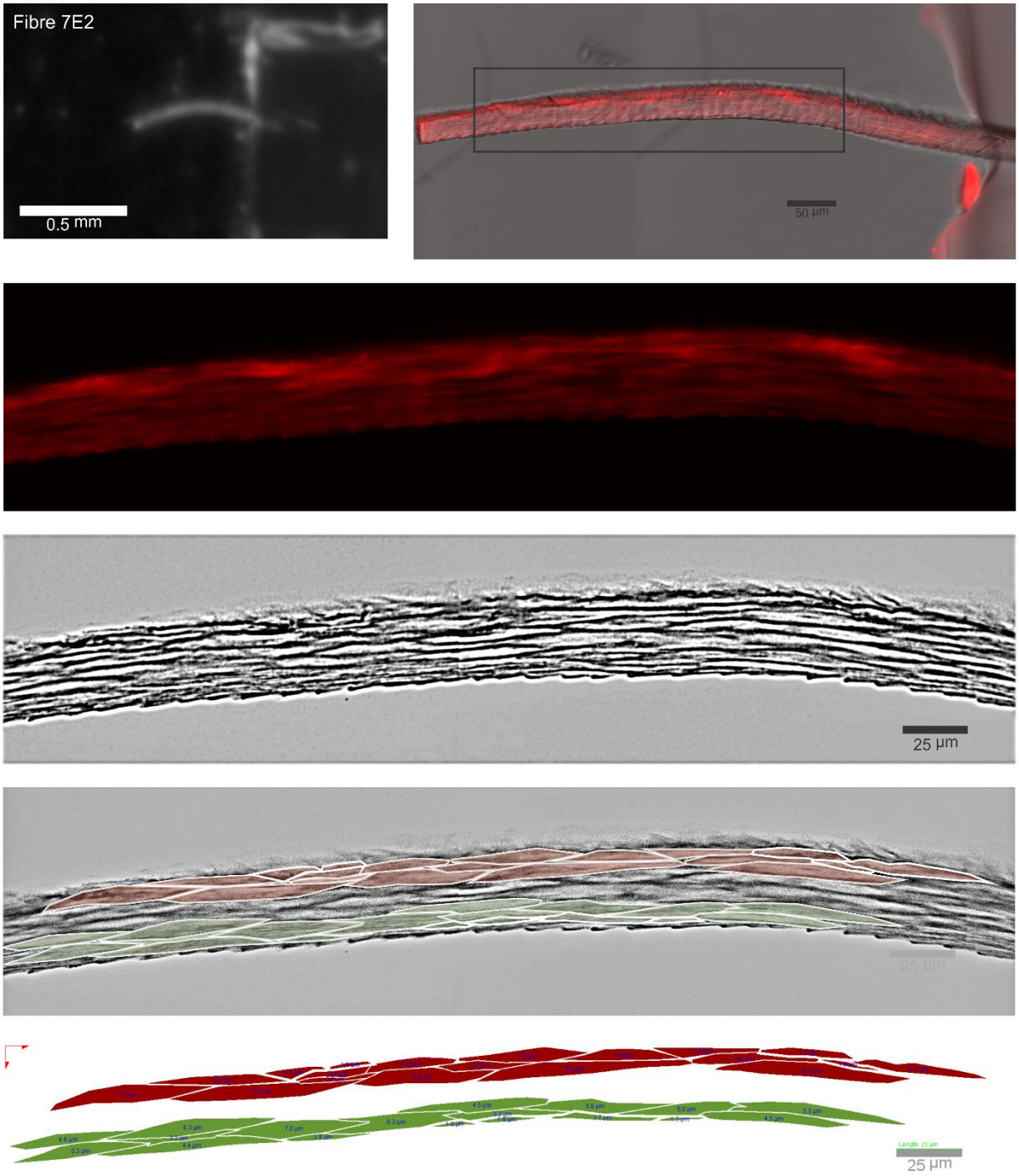

Fig. S4. Example images from preliminary work carried out to determine sampling approach. This included non-linear changes to contrast and local contrast enhancement methods. Cells taken within two cell widths from the fibre surface ensured that cell type could be determined. Centrally located cells were less easy to identify unambiguously.

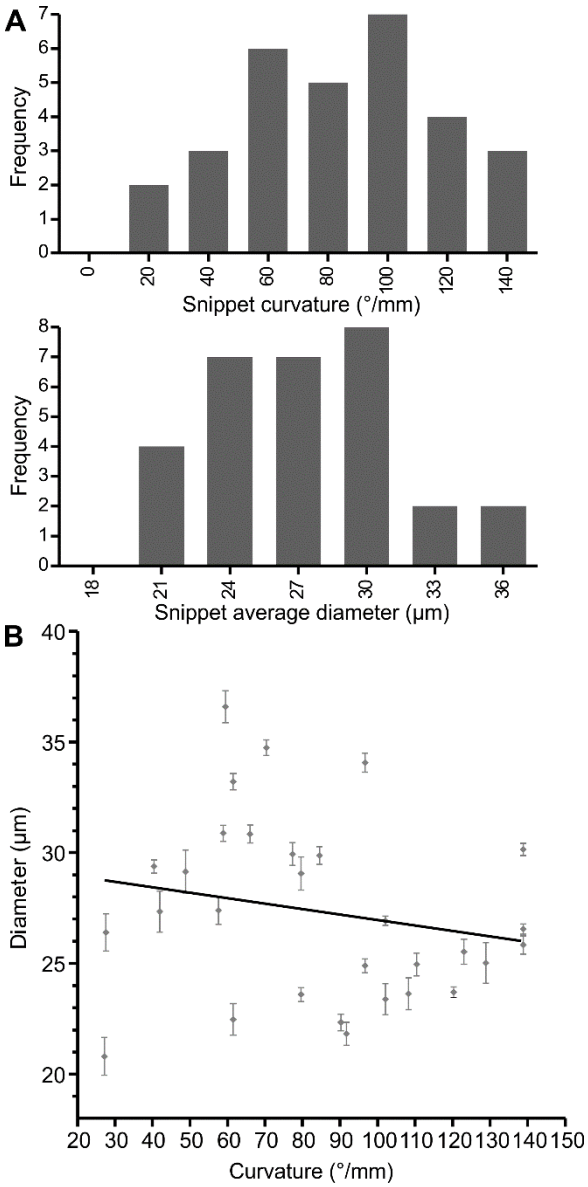

Fig. S5. Range of curvatures and diameters of snippets used in the cell-type analysis. A. distributions of curvatures and diameters. B. Diameter plotted against curvature for all snippets as means of 5 x-z sections per snippet, error bars are standard error of the mean and line is a linear regression.

Table S2. Regressions of data from orthocortex/paracortex analysis (n = 30 snippets x 5 x-z sections per snippet). CSA is cross-sectional area. NS is non-significant.

Relationship	Linear regression (r^2)	Deviation from zero slope	Figure
Diameter and curvature	0.04	NS	Sup.Fig.5B
CSA orthocortex and diameter	0.75	P<0.0001	Figure 3A
CSA paracortex and diameter	0.69	P<0.0001	Figure 3A
CSA orthocortex and curvature	0.00	NS	Figure 3B
CSA paracortex and curvature	0.08	NS	Figure 3B
Orthocortex paracortex ratio and curvature	0.02	NS	Figure 4A
CSA orthocortex minus paracortex as a proportion snippet CSA and curvature	0.06	NS	Figure 4B
Distance between centres of mass of orthocortex and paracortex	0.01	NS	Figure 4C
Distance between central points normalised by diameter of snippet	0.07	NS	Figure 4D
Orthocortex convexity and curvature	0.10	NS	Figure 5A
Paracortex convexity and curvature	0.01	NS	Figure 5A
Orthocortex aspect ratio and curvature	0.01	NS	Figure 5B
Paracortex aspect ratio and curvature	0.42	NS	Figure 5B
Cortex aspect ratio and curvature	0.05	NS	Figure 5B
Orthocortex circularity and curvature	0.01	NS	Figure 5C
Paracortex circularity and curvature	0.10	NS	Figure 5C
Cortex circularity and curvature	0.02	NS	Figure 5C

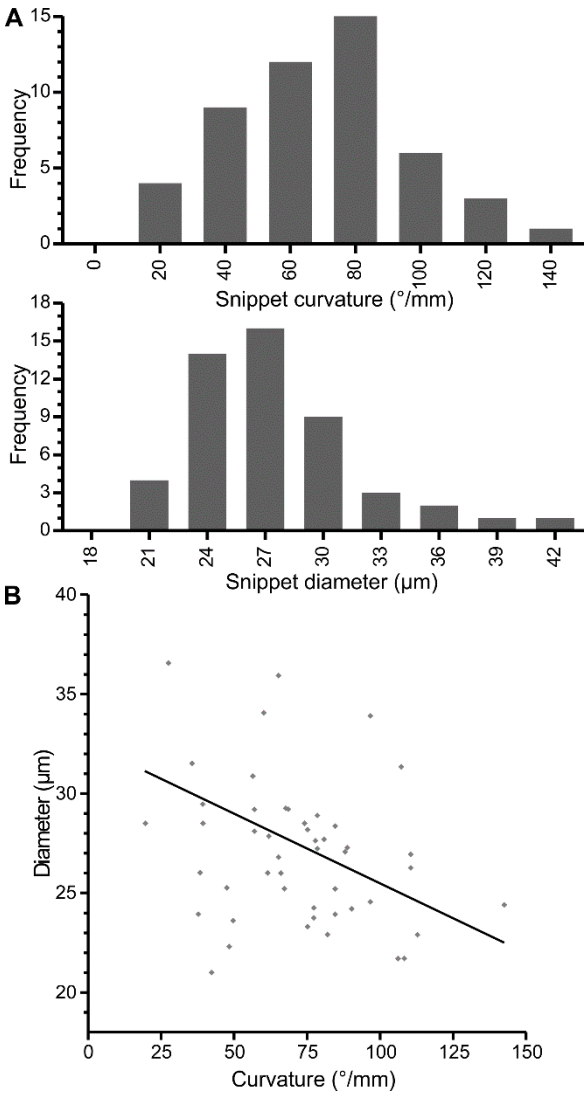

Fig. S6. Range of curvatures and diameters of snippets used in the cell-length analysis. A. distribution of curvatures and diameters. B. Diameter plotted against curvature for all snippets. The line is a linear regression.

Table S3. Regressions of data from cell length/number analysis (n = 50 snippets).

Relationship	Linear regression (r^2)	Deviation from zero slope	Figure
Diameter and curvature	0.18	P<0.0025	Sup.Fig.6B
Outside cell length and fibre diameter	0.14	P<0.01	Figure 7A
Inside cell length and fibre diameter	0.22	P<0.001	Figure 7A
Pooled cell length and fibre diameter	0.21	P<0.001	Figure 7A
Outside cell length and fibre curvature	0.01	NS	Figure 7B
Inside cell length and fibre curvature	0.13	P=0.013	Figure 7B
Pooled cell length and fibre curvature	0.02	NS	Figure 7B
Outside to inside cell length difference and curvature	0.30	P<0.0001	Figure 7C
Outside to inside cell length difference divided by fibre diameter, and fibre curvature	0.42	P<0.0001	Figure 7D
Ratio of number of cells in 250 µm, outside:inside and fibre diameter	0.02	NS	Figure 8A
Ratio of number of cells in 250 µm, outside:inside and fibre curvature	0.23	P<0.001	Figure 8B